energies

MDPI

Article

A Novel Approach to Transverse Flux Machine Construction

Tomasz Drabek [1], Piotr Kapustka [2], Tomasz Lerch [1,*] and Jerzy Skwarczyński [1]

[1] Faculty of Electrical Engineering, Automatics, Computer Science and Biomedical Engineering, AGH University of Science and Technology, 30-059 Krakow, Poland; drabek@agh.edu.pl (T.D.); jskw@agh.edu.pl (J.S.)
[2] Department of Electrical Engineering, Polytechnic Faculty, PWSZ University of Applied Sciences in Tarnow, 33-100 Tarnow, Poland; p_kapustka@pwsztar.edu.pl
* Correspondence: lerch@agh.edu.pl; Tel.: +48-12-617-4016

Abstract: The article presents a concept for a new design of the well-known Transverse Flux Machine (TFM) made with the use of a flat core used in classical electrical machines. The proposed design was first analytically verified and was subsequently verified using the finite element method, which fully corroborated the results. The simulations show that a set of three single-phase TFM machines with slotted flat rotor yokes generates a torque over three times greater than that of an induction motor and twice as large as Fractional Slot Concentrated Winding—Permanent Magnet Synchronous Machines (FSCW-PMSM). The performed comparative calculations confirmed that the torque generated by machines operating on principles similar to TFM can generate a torque much greater than those currently in common use.

Keywords: transverse flux machine; permanent magnet synchronous motor; induction motor

Citation: Drabek, T.; Kapustka, P.; Lerch, T.; Skwarczyński, J. A Novel Approach to Transverse Flux Machine Construction. *Energies* **2021**, *14*, 7690. https://doi.org/10.3390/en14227690

Academic Editors: Ants Kallaste and Lorand Szabo

Received: 24 September 2021
Accepted: 13 November 2021
Published: 17 November 2021

1. Introduction

There is always strong interest in new designs of electrical machines due to the desire to increase the power and torque unit indicators. One way in which this goal can be achieved is through the elimination or at least shortening of the winding front connections. These connections do not participate directly in the energy conversion process, but they are necessary for generating a rotating field during the operation of machines based on the use of this field. TFMs, however, use a completely different operating principle, resulting in the complete absence of front connections.

The design of an electrical machine with a transverse flux was patented in 1888 [1], and almost a hundred years later it was adapted to modern technical capabilities and technologies [2]. Over the past 30 years, much research work has been devoted to TFMs, e.g., [3–5].

Numerous advantages of this construction have been demonstrated, the most important of which is the much greater ratio of mass and volume to power than exists in other machines. Despite this, TFMs are not widely used and produced at present, probably due to several disadvantages in their construction, the most serious of which are:

- the complicated design and, as a result, higher production costs and reduced reliability;
- the relatively low use of permanent magnet surfaces, which results in large leakage fluxes;
- the large cogging torque.

Since the transverse flux machine is an extremely interesting object from the perspective of the theory of electrical machines, it was considered useful to compare some of its properties with the corresponding features of induction machines and Fractional Slot Concentrated Winding—Permanent Magnet Synchronous Machines (FSCW-PMSM), which are in common use. Over the past 20 years, a series of studies have been published describing their features and performance [6,7].

Transverse flux machines have a construction containing electromagnetic circuits in which the lines of force mediating the energy conversion remain in a plane perpendicular to the direction of the motion [2,8]. Figure 1 schematically shows the construction of the prototype motor in its most basic form, designed in order to conduct laboratory tests [9].

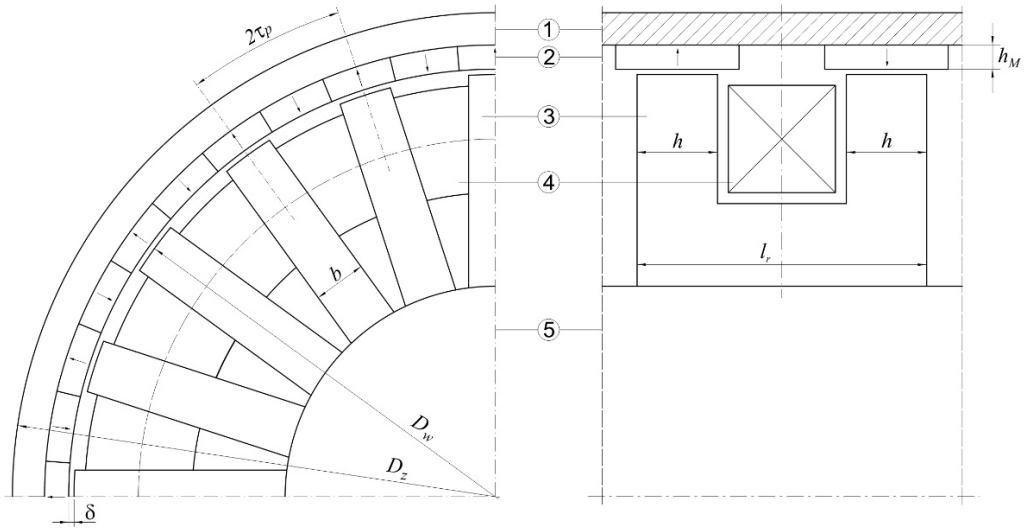

Figure 1. Cross-section and longitudinal section of the transverse flux machine (TFM) basic version: 1—outer steel cylinder, 2—permanent magnets, 3—armature components—U cores, 4—winding ring, 5—hub/shaft.

The movable element is the steel cylinder 1, external to the armature, with permanent magnets 2 placed on its inner surface. The armature consists of a winding ring 4 with cores 3 covering the winding. The poles dimensions in Figure 1 are: h—width in the axial direction, b—thickness in the circumferential direction, h_M—height. The distance of armature elements (inverted U-shaped cores) in the circumferential direction is $2\tau p$, where τp—pole pitch in the circumferential direction. The angular span of the armature cores should be equal or slightly smaller than the angular span of the magnets (in the presented structure it is smaller, $b < \tau p$). The armature winding has the form of a ring wound in a plane perpendicular to the axis of rotation. The air gap δ allows the winding to move along with the cores relative to the magnets. Armature cores comprise packages of sheets.

The following engine dimensions were adopted for the simulation: the outer diameter of the rotor yoke D_z = 0.152 m; the outer diameter of the cylindrical surface of the armature D_w = 0.133 m; the air gap $\delta = 8.4 \times 10^{-4}$ m; the height of the magnets h_M = 0.0038 m; the dimensions of the armature cores: b = 0.008 m; h = 0.0127 m; the core window 0.02 × 0.02 m; the axial dimension of the core l_r = 0.0454 m; the permanent magnet used: μ_{pmr} = 1.045; H_C = 883,310 A/m.

The arrangement of elements and the relationships between individual dimensions were taken from [9], including the assumption that the dimensions of the system of three single-phase units must not exceed the external dimensions of the winded stator of the 2.2 kW squirrel-cage induction motor, which is treated as comparative. Therefore, the diameter of the outer ring with magnets D_z = 152 mm was taken as equal to the outer diameter of the 2.2 kW motor stator yoke. However, the axial dimension of U cores with spaces could not be greater than the value of 170 mm, which is close to the axial dimension of the winding of induction motor package of this size.

The value determining the motor's properties is the linkage flux of the winding ring, which is produced by permanent magnets. The flux is the sum of magnetic field lines running along the axial fragments of individual U cores. The Finite Element Method (FEM) 2D software was used to determine this flux and its changes caused by the rotor movement, wherein treating the magnetic field in TFM as "flat" is only allowed in limited parts of the machine. A fragment of a two-dimensional model of the field excited using permanent

magnets is shown in Figure 2. It consists of a cross-section of cores and magnets (Figure 1) with the plane perpendicular to the axis of rotation. The cross-sectional plane runs along the radial axis of the U core sections located on one side of the armature winding.

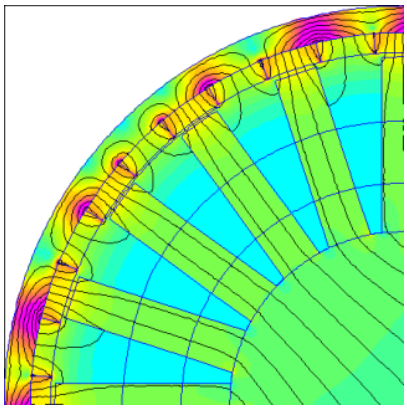

Figure 2. Finite Element Method (FEM) model of a TFM machine used to calculate flux changes during rotor rotation.

It was assumed that the sought flux value in the axial section of the core is equal to the flux in the radial section of the core, close to the transition to the axial section. In the "flat" field for the radial section, this can be expressed as:

$$\phi_{pm} = h\,\Delta A_{pm} \tag{1}$$

wherein h—the pole width in the axial direction (Figure 1), ΔA_{pm}—the difference of vector potentials at two selected points outside the core poles [Vs/m].

In the case under consideration, ΔA_{pm}, it may be called the core flux per unit of its axial dimension, or the unit core flux. Figure 3 shows the course of changes in the unit flux with a solid blue line ΔA_{pm} in the core as the rotor rotates by two pole graduations. The amplitude of the first harmonic of the waveform $\Delta A_{pm}(\varphi)$ is $3.5 \cdot 10^{-3}$ Vs/m, while the amplitude of the third harmonic is 3.7% of the first, and the others are below 1%.

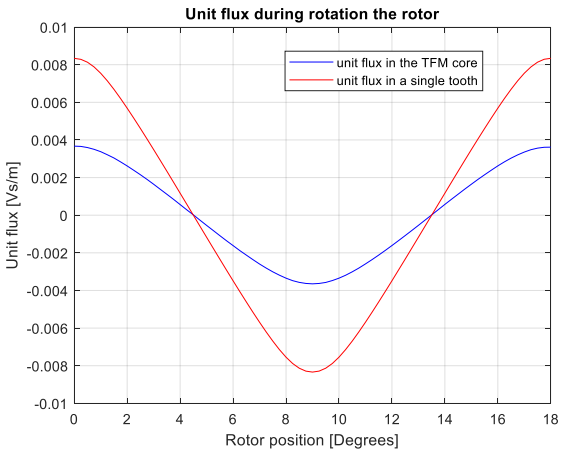

Figure 3. Unit flux changes as the rotor turns 18 degrees.

In Figure 4, the blue line represents the drawn distribution of the radial induction component in the center of the width of the air gap between the magnets and the core pole U, and the average value of this induction. The induction in the core cross-section for which the flux was calculated can be considered a constant. It is 0.42 T; hence it is almost half of the average induction in the air gap (0.78 T). The reason for this difference is the

flux leakage, the lines of which close between the exposed surfaces of the magnets and the sides of the radial sections of the U core.

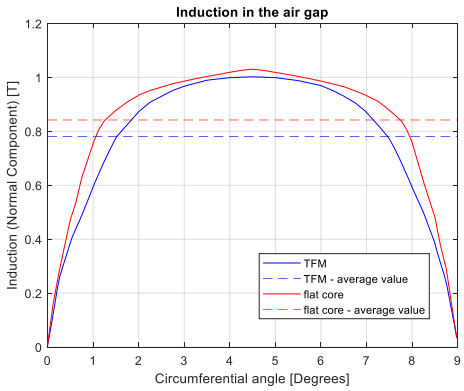

Figure 4. Comparison of the radial component of induction at half the air gap width for classic TFM and flat core design.

2. Methods to Reduce Leakage Flux

To reduce the leakage flux, the magnets' free surfaces must be limited. There are numerous proposed methods to achieve this, some of which are presented in Figure 5. The "oblique" orientation of the cores can be considered the simplest solution, i.e., orienting them in such a way that the ends of each U core are above two successive elements in a single row of magnets, and not one pair of magnets coming from two parallel series as in Figure 1. This requires a corresponding increase in the axial dimension of the magnet ring. An illustrative version of this solution is shown in Figure 5a originating from [10]. The author presents the magnetic flux path in a single-sided transverse flux machine with twisted stator cores and external rotor permanent magnets. A further development of the method was to provide each end of the core with a trapezoidal ending, i.e., a claw—the idea being to focus the maximum amount of force lines coming out of the magnet on the crevice surface of the core. Instead of surface magnets, as in the structure shown in Figure 5a, the excitation element is a ring composed of permanent magnets and ferromagnetic inserts. These elements of the ring act as a flux concentrator [1]. The layout is easier to see in Figure 5b [11], which also shows another version of the oblique poles according to [12].

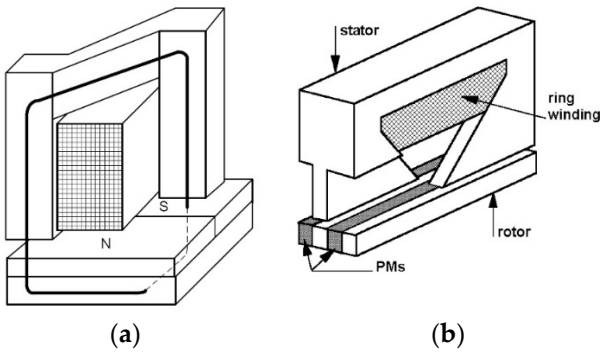

Figure 5. Proposed methods of the flux leakage reduction presented in publications: (**a**)—twisted stator cores [10] © [2005] IEEE. Reprinted, with permission, from [Gieras, J.F. Performance Characteristics of a Permanent Magnet Transverse Flux Generator. In Proceedings of the IEEE In-ternet Conference on Electric Machines and Drives, San Antonio, TX, USA, 15 May 2005; pp. 1293–1299. IEEE Industry Appli-cations Society], (**b**)—flux-concentration and twisted stator cores [11,12] © [2004] IEEE. Reprinted, with permission, from [Masmoudi, A.; Njeh, A.; Mansouri, A.; Trabelsi, H.; Elantably, A. Optimizing the Overlap Between the Stator Teeth of a Claw Pole Transverse-Flux Permanent-Magnet Machine. IEEE Trans. Magn.].

Cores designed for "oblique" as well as "transverse" alignment are situated in the changing magnetic field while the machine is moving and cannot be solid. Due to the difficulty of using magnetic core sheets, they have to be made of metal powders. However, the use of oblique poles does not eliminate the leakage flux, even after using the hub, and only reduces its impact at the expense of the emergence of a significant construction complication. It can also be seen that when the positions of the cores are changed, the structure formally ceases to be a machine with a transverse flux.

3. The Use of a Flat Core

A traditional slotted flat core can be considered a series of oblique U cores rotated 90 degrees from a transverse position, as in Figure 5a. The winding inserted into such a core can no longer be a flat ring but must consist of fragments in slots and frontal connections. It can also be formed of coils wound around individual teeth, then connected in a series. This solution doubles the flux linkage with the winding.

Replacing the U armature cores with a traditional slotted cylindrical core causes the leakage flux to be radically reduced, but the winding length increases and the cross-section of the winding is limited by the dimensions of the slot. Because flat cores with a number of slots equal to the number of magnet poles are not used due to the large cogging torque, the operation of such a construction was simulated. The principle of generating torque is identical as in the TFM. The cross-section is shown in Figure 6. In an unchanged outer steel ring, only one row of magnets was left, with their axial dimension increased to the combined dimension of both rows. The length of the slotted core packet was assumed to be equal to the axial dimension of the U cores. The axial dimensions of the magnets and the core were aligned, preserving the radial dimension of the air gap. It was assumed that the field in such a layout can be treated as flat. Figure 7 shows the shape of the force lines of the field excited by magnets.

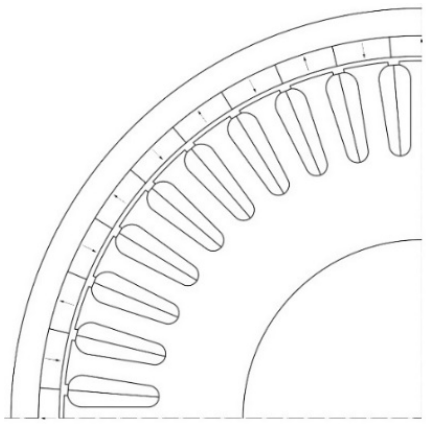

Figure 6. The cross-section of a flat core construction proposed in this article.

The coils cover individual teeth and are connected alternately in a series. In the de-energized state of the coils, each pair of teeth is influenced by the same magnetomotive force (MMF) of magnets as each U core. Assuming no leakage flux and the linearity of the cores, the flux in the teeth should remain at the same level as the flux in the U cores. Under these conditions, in the circuit made of coils, where the total number of turns is the same as in the ring winding in Figure 1, a similar electromotive force (EMF) value should be induced while the rotor is moving. The leakage flux, however, reduces the flux in the U cores as it moves away from the magnets; thus the EMF in the circuit composed of the coils around the teeth will be higher than in the winding loop of the TFM.

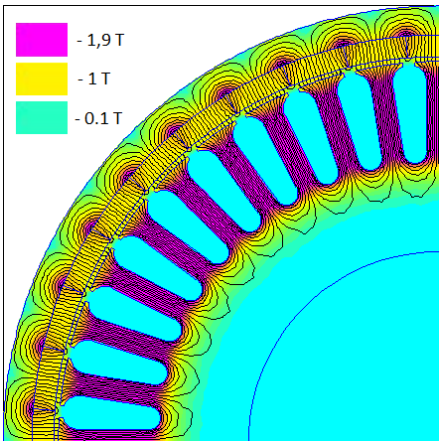

Figure 7. The shape of magnetic lines forces in a proposed flat core design.

In Figure 3, the solid red line shows the course of the unit flux of a single yoke tooth when the rotor rotates by two polar pitches. The amplitude of the flux is more than twice as large as in the U core, while the radial component of the induction at half the width of the air gap in both structures is similar—see Figure 4, red and blue horizontal lines.

4. Estimation of the Torque

The main component of the torque developed in a single-phase electromagnetic system excited by permanent magnets for most structures equals [13]:

$$T_e = i \frac{\partial \psi_{pm}}{\partial \varphi} \tag{2}$$

where i—the winding current, ψ_{pm}—the winding linkage flux in a currentless state.

Flux ψ_{pm} is a periodic function of the angle of the rotor φ; if its changes are close to a sine wave, it can be represented by the formula:

$$\psi_{pm}(\varphi) \approx \Psi_{pmm1} \cos p_b \varphi \tag{3}$$

wherein the position of the rotor is $\varphi = \omega t + \varphi_o$. The symbol p_b represents the number of pole pairs of magnets, Ψ_{pmm1}—amplitude of the first harmonic of flux changes $\psi_{pm}(\varphi)$.

To obtain a mean value of the torque different from zero, the winding current should be a similar function of time:

$$i(t) = I_m \sin(\omega_o t + \zeta) \tag{4}$$

Then:

$$T_e = -p_b I_m \Psi_{pmm1} \sin(\omega_o t + \zeta) \sin p_b \varphi \tag{5}$$

To obtain the mean value of the torque, the pulsation of the current ω_o must be related to the instantaneous speed of the machine ω according to the formula resulting from the relationship:

$$\omega_o t = p_b \varphi = p_b \omega t \tag{6}$$

For the current pulsation $\omega_o = p_b \omega$ and the compatible EMF, as well as the current phases, the average value of the torque is:

$$T_{eav} = \frac{1}{2} p_b I_m \Psi_{pmm1} \tag{7}$$

Other torque components, including the cogging torque, have been neglected.

4.1. Single-Phase TFM—Primary Construction

If the winding is concentrated (Figure 2), the linkage flux of the winding is $\psi_{pmA} = p_b z_{uA} \phi_{pmA}$ where p_b—the number of armature U cores equal to the number of pole pairs of magnets, z_{uA}—the number of the coil turns, ϕ_{pmA}—the flux in the axial section of the core length h according to (1): $\phi_{pmA} = h \Delta A_{pmA}$, where ΔA_{pmA}—the difference of vector potentials A_{pmA} at two selected points outside the poles of the core of the "A" structure. The amplitude of the first harmonic of the flux changes $\psi_{pmA}(\varphi)$ and the number of the coil turns can be represented by the formula:

$$\Psi_{pmm1A} = p_b z_{uA} h \Delta A_{pm1A} \tag{8}$$

The symbol ΔA_{pm1A} marks the first harmonic of changes in the unit flux of the "A" structure.

The current I_{mA} (maximum value) can be replaced by the product:

$$I_{mA} = j_A S_{CuA} = j_A k_{wzA} S_{uA} \frac{1}{z_{uA}} \tag{9}$$

wherein the respective symbols denote: j_A—the current density, S_{CuA}—the single conductor cross-section, k_{wzA}—the factor of filling the surface of a single slot S_{uA} provided for the winding with turns. In the case under consideration, S_{uA} is the area of the rectangle between the poles of the core (U core window area in Figure 1).

After substituting (8) and (9) with (7), the expression for the average value of the torque produced by one segment of classic TFM (one phase) is obtained:

$$T_{eavA} = \frac{1}{2} p_b I_{mA} \Psi_{pmm1A} = \frac{1}{2} k_{wzA} j_A S_{uA} h p_b^2 \Delta A_{pm1A} \tag{10}$$

4.2. Single-Phase System with Slotted Core and Concentrated Coils—Proposed Structure

If the circuit is formed from identical series of connected coils wound around each tooth of the core (Figure 6), wherein the number of teeth is equal to the number of poles of the magnets, the linkage flux of the winding in the currentless state with a full symmetry of the circuit is: $\psi_{pmB} = 2 p_b z_{cB} \phi_{pmB} = z_{uB} \phi_{pmB}$, wherein $2p_b$—the number of armature coils is equal to the number of poles of the magnets, z_{cB}—the number of turns of the coil, ϕ_{pmB}—the flux in the axial section of the core according to (1): $\phi_{pmB} = l_{Fe} \Delta A_{pmB}$. The amplitude of the first harmonic of the flux changes $\psi_{pmB}(\varphi)$ can be represented by the formula:

$$\Psi_{pmm1B} = p_b z_{uB} l_{Fe} \Delta A_{pm1B} \tag{11}$$

The symbol ΔA_{pm1B} marks the first harmonic of changes in the unit flux in the middle section of the tooth.

The current I_{mB} (maximum value) can be replaced by the product:

$$I_{mB} = j_B S_{CuB} = j_B k_{wzB} \frac{1}{2} S_{uB} \frac{1}{z_{uB}} \tag{12}$$

wherein the respective symbols denote: j_B—the current density, S_{CuB}—the single conductor cross-section, k_{wzB}—the factor of filling the surface of a single slot S_{uB} provided for the winding with turns.

After substituting (11) and (12) with (7), the expression for the average value of the torque produced by one segment of the proposed structure (one phase) is obtained:

$$T_{eavB} = \frac{1}{2} p_b I_{mB} \Psi_{pmm1B} = \frac{1}{2} k_{wzB} j_B S_{uB} p_b^2 l_{Fe} \Delta A_{pm1B} \tag{13}$$

The relationship between the mean values of torques T_{eavA} and T_{eavB} is defined by the quotient:

$$\frac{T_{eavA}}{T_{eavB}} = \frac{k_{wzA}\, j_A\, S_{uA} h\, \Delta A_{pm1A}}{k_{wzB}\, j_B\, S_{uB} l_{Fe}\, \Delta A_{pm1B}} \tag{14}$$

Assuming the same current density and the same slot filling with copper, we will get:

$$\frac{T_{eavA}}{T_{eavB}} = \frac{S_{uA}}{S_{uB}} \frac{h}{l_{Fe}} \frac{\Delta A_{pm1A}}{\Delta A_{pm1B}} \tag{15}$$

For the TFM dimensions presented above and the assumed dimensions of the cylindrical core, the slot cross-section is S_{uB} = 80.5 mm^2 and for the core length l_{Fe} = 40 mm, we get:

$$\frac{T_{eavA}}{T_{eavB}} = \frac{20 \times 20}{80.5} \frac{12.7}{40} \frac{3.5 \cdot 10^{-3}}{7.8 \cdot 10^{-3}} = 5 \cdot \frac{1}{3.15} \frac{1}{2.2} = 0.7 \tag{16}$$

The difference between the torques can be reduced by design measures, in particular by reducing the leakage fluxes in the machine with a transverse flux. The difference will also vary for the various TFM variants already proposed. Both presented single-phase constructions can thus be "roughly" regarded as equivalent.

If we assume, as in the case of an induction motor, a power of 2.2 kW, the slot filling factor k_{wz} = 0.35 and the current density j = 6.5 A_{sk}/mm^2, the value of the torque generated by the classic design TFM according to (10) is:

$$T_{eavA} = \tfrac{1}{2}\, j_A k_{wzA}\, S_{uA} h\, p_b^2 \Delta A_{pm1A} = \tfrac{1}{2} 6.5 \cdot \sqrt{2} \cdot 0.35 \cdot 411 \cdot 0.01267 \cdot 20^2 \cdot 3.5 \cdot 10^{-3} = \\ = 11.7\,\text{Nm}$$

The torque produced in the system with a traditional (slotted) core, according to (13), is:

$$T_{eavB} = \tfrac{1}{2}\, j_B k_{wzB} S_{uB} p_b^2 l_{Fe} \Delta A_{pm1B} = \tfrac{1}{2} 6.5 \cdot \sqrt{2} \cdot 0.35 \cdot 80.5 \cdot 20^2 \cdot 0.04 \cdot 7.8 \cdot 10^{-3} = \\ = 16.2\,\text{Nm}$$

In Figure 8, the blue line shows the changes in T_{eB} torque, produced by one segment of the proposed construction, when rotating the rotor under the conditions of supplying the winding with alternating current, in phase with the EMF. FEM calculations were made using the FEMM 4.2 software. The horizontal blue line shows the average T_{eB} torque value. It amounts to 16 Nm; hence it is close to T_{eavB} determined according to (13). Taking into consideration the nonlinearity of the core, the magnetization characteristic reduces the average torque value to 14.5 Nm, i.e., approx. 10%—the horizontal red line in Figure 9. The same figure also shows the dependence of the torque on the position of the rotor, taking into consideration the saturation of the core—the red curve. Except for the mean value, torque has a large variable component. Theoretically, its amplitude should be equal to the average value; however, the influence of the cogging torque is visible, which causes a periodic change of the sign of the torque.

Figure 9 shows the first harmonics of the EMF induced in the armature winding resulting from the permanent magnets (solid blue line), the linkage flux with the armature winding under load (solid black line) and the armature flux impact (solid red line). The dotted blue curve corresponds to the voltage waveform on the armature resistance, magnified 10 times. For the assumed number of turns in one coil—8—the rated armature current is 11.5 A (root mean square (RMS) value), and the resistance of the entire winding is 0.44 Ω. For a rotational speed of 1500 rpm, the RMS value of EMF induced by the winding flux linkage is 226 V, with the phase angle between this EMF and the current of 10.8 degrees. This corresponds to the produced torque of 16.2 Nm, hence a value very close to the one previously determined (for the linear magnetization characteristic of the cores). The machine is characterized by its very low armature impact and very good power factor.

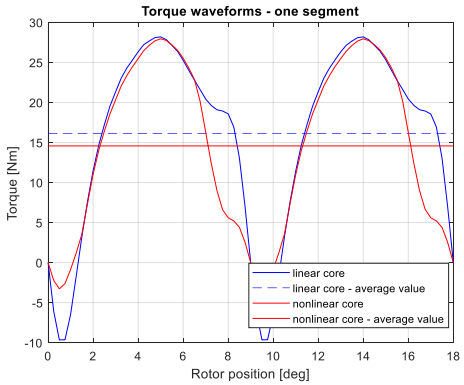

Figure 8. Comparison of torque waveform as a function of rotor position angle for the linear core and nonlinear core.

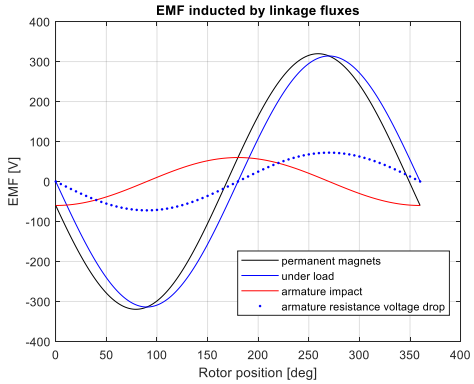

Figure 9. First harmonics of EMF induced by linkage fluxes in the proposed flat core design.

5. Three-Phase System

A set of three single-phase systems of slotted flat cores placed on a common shaft with magnets shifted circumferentially by the "electric" angle $2\pi/3$, powered by three-phase currents, will increase the mean torque by a factor of three and thereby radically reduce its variable component—see Figure 10. As it can be seen from the previous calculations, one segment of the set produces an average torque of 14.5 Nm (considering saturation), so a set of 3 segments with a total axial dimension $L_o \approx 0.17$ m, will generate a torque of 3–14.5 Nm = 43.5 Nm. With a pulsation of 3-phase currents $\omega_o = 1000\pi$ s^{-1} (500 Hz) it will issue power 1000π s^{-1}·43.5 Nm/20 $\approx$ 6.8 kW for 1500 rpm, thus more than 3 times larger than a squirrel-cage induction motor with an electromagnetic circuit of the same dimensions.

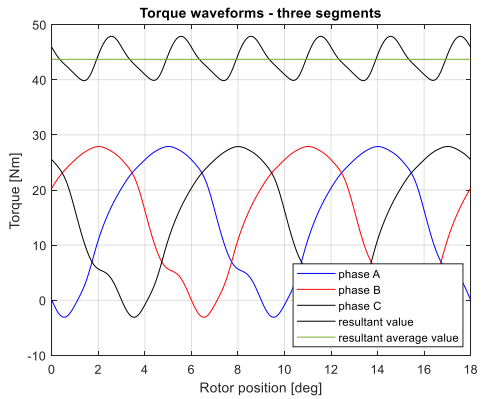

Figure 10. Torque waveforms for three segments and their resultant values.

The diameter of the outer ring with magnets was assumed for each segment as D_z = 152 mm, the core pack length of l_{Fe} = 40 mm and the axial dimension of the coils including the front connections as l_c = 40 mm + 2·6 mm = 52 mm. Assuming a spacing of 7 mm between the segments, the axial dimension of the set of 3 single-phase systems will be L_o = 3·52 mm + 2·7 mm = 170 mm, which is close to the axial dimension of the wound motor package 2.2 kW. A demonstrative drawing of the proposed 3-phase construction is shown in Figure 11. The disadvantage of the machine will be the high cogging torque, which will cause noticeable speed fluctuations at low rotational speeds and a small moment of inertia of the driven system. The problem of the TFM cogging torque reduction is quite widely described in the literature, e.g., [14–17].

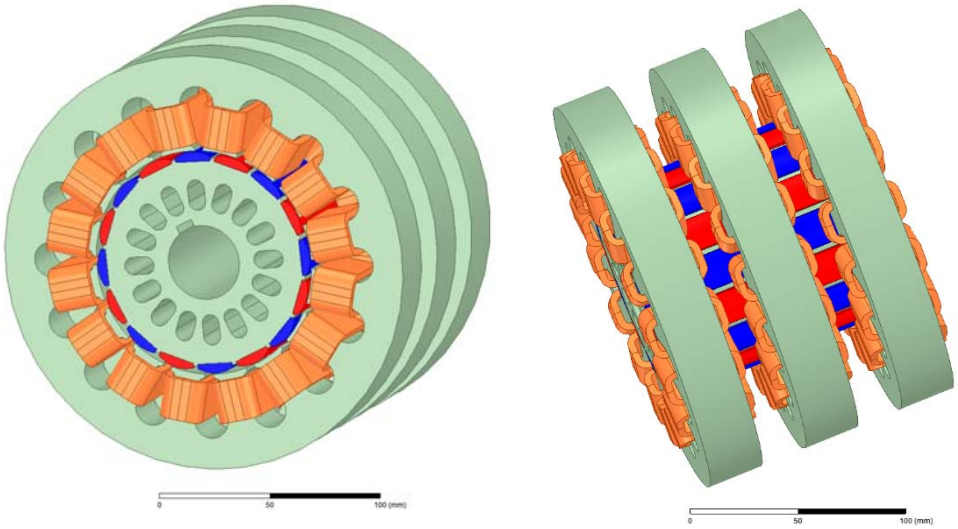

Figure 11. Demonstrative drawing of the proposed three-phase construction.

The structure presented in Figure 6 visually resembles the commonly used multipolar synchronous machines with concentrated fractional windings excited by permanent magnets, e.g., [18]. However, they have a multiphase armature and different armature groove pitches and polar excitation. The difference is selected so that in each of the windings made of coils connected in series, EMF are induced, shifted by the angle required for the assumed number of phases. In particular, for example, for the number of poles—40—the closest required number of teeth/ yoke coils would be 36. These designs are widely used and thoroughly tested as Fractional Slot Concentrated Winding—Permanent Magnet Brushless DC (FSCW PMBLDC) and AC motors. A fragment of a cross-section of such a machine is shown in Figure 12.

Reducing the number of slots enables the slot cross-section to be increased to S_z = 103 mm^2. For a core package with a length of l_{Feg} = 0.158 mm, the core dimension together with the short frontal connections around the tooth coils (2 × 6 mm) is close to the total axial dimensions $L_o \approx 0.17$ m of the single-phase core set. The torque generated by such a machine is 23 Nm. Calculations considering saturation, performed in accordance with the FEM method, showed a small variable component, within the range of ±3.3% of the mean value—see Figure 13.

Thus, in a construction with a three-phase armature, the torque is almost two times lower than that produced by three single-phase systems with slotted flat cores, but the cogging torque is incomparably smaller.

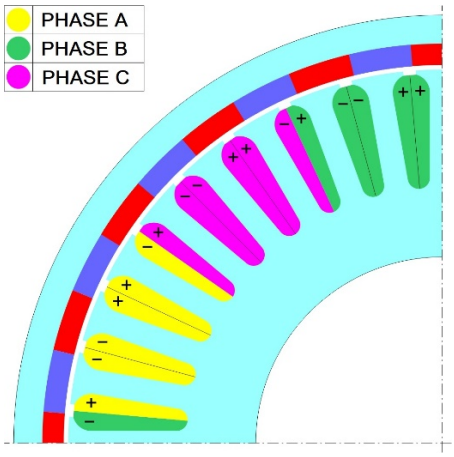

Figure 12. Fragment of a cross-section of a 3-phase FSCW-PMSM machine with 40 poles and 36 teeth-coils.

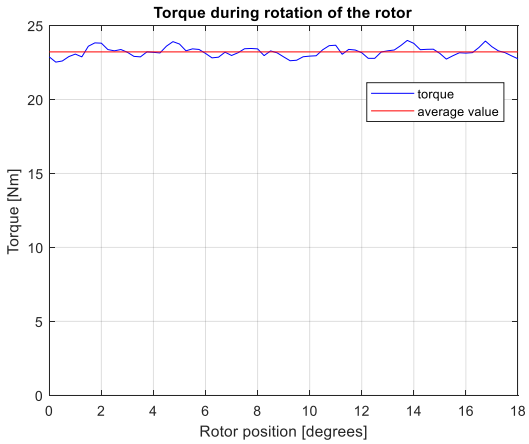

Figure 13. Torque calculations of a Fractional Slot Concentrated Winding—Permanent Magnet Brushless DC (FSCW PMBLDC) machine with 40 poles and 36 teeth-coils considering saturation.

6. Comparison with an Induction Motor

The torque produced by a 2.2 kW squirrel-cage induction motor at a rated speed of 1435 rpm is 14.6 Nm with a power factor of 0.74. The outer diameter is 152 mm, while the axial dimension of the stator package is 95 mm. The dimensions are determined by the diameter and axial dimensions of the wound stator and are thus considered together with the winding front connections. The relation of this dimension to the length of the core varies, depending on many factors, from 1.2 to as high as 2. In the considered motor, it is 48 mm on each side of the core. In low-power motors, the frontal connections usually extend the machine by 60–80%; hence the reference dimension was taken as L_o = 170 mm.

The simulation shows that the commonly used FSCW-PMSM, without any optimization procedures carried out at the design stage, can produce 23 Nm, which is 50% more than the squirrel-cage motor. A set of 3 single-phase machines with slotted flat rotor yokes produces a torque of 48 Nm, which is more than 3 times greater than that of an induction motor and twice as large as that of the FSCW-PMSM. This is also how the torque produced by the TFM should be assessed. However, the average torque value is superimposed by high cogging torques with a pulsation of $2p_b\omega$. The values of the torques generated by individual constructions obtained from the simulation are compared with the rated torque of the induction motor in Table 1.

Table 1. Summary of the torque generated by individual constructions.

	Induction Motor	**FSCW-PMSM**	**3 TFM with Toroidal Windings**	**3 Segments with Flat Cores**
T_{av} [Nm] for l_{Fe} = 0.095 m	14.6 (1435 rpm/min)	13.8	3 × 11.7 = 35.1	3 × 14.5 = 43.5
T_{av} [Nm] for l_{Feg}	—-	23	—-	—-
T_{zm} [% T_{sr}]	—-	±3.5	—-	±9

7. Conclusions

It is widely assumed that one of the great advantages of transverse flux machines is that there is no direct correlation between the dimensions of the winding cross-section and the dimensions of the main magnetic circuit. In traditional machines, the enlargement of the winding cross-section takes place at the expense of reducing the area through which the magnetic field lines of force close and vice versa; in the TFM, these dimensions are independent of each other. The presented analyses show that, within the given dimensions, the range of changes in the dimensions of electric and magnetic circuits is limited, and the dimensions are largely interdependent. The comparative calculations performed confirmed that the torque generated by machines operating on principles similar to the TFM can be much greater than the torque generated by machines currently in common use. However, the cogging torques accompanying the operation of the machine need to be reduced by special design treatments.

Because segmented machines are only used to a limited extent due to their higher production costs, it can be predicted that the TFM will remain a machine dedicated for use in drives where generating great torque in the smallest possible volume is required, e.g., on ships or in wind farms. A patent application for the described design of the TFM motor has been filed and is pending [19].

Author Contributions: Conceptualization, J.S. and T.D.; methodology, T.D.; software, J.S.; validation, T.D. and T.L.; formal analysis, T.D.; investigation, P.K.; resources, P.K.; data curation, T.D.; writing—original draft preparation, J.S. and T.L.; writing—review and editing, P.K. and T.L. All authors have read and agreed to the published version of the manuscript.

Funding: This research was funded by the AGH University of Science and Technology, research subsidy no. 16.16.120.7998.

Institutional Review Board Statement: Not applicable.

Informed Consent Statement: Not applicable.

Data Availability Statement: The data presented in this study are available on request from the corresponding author.

Conflicts of Interest: The authors declare no conflict of interest.

References

1. Mordey, W.M. Electric Generator, No. 5162. U.S. Patent 437501, 30 September 1890.
2. Weh, H.; May, H. Achievable Force Densities for Permanent Magnet Excited Machines in New Configurations. In Proceedings of the Internet Conference Electrical Machines (ICEM86), München, Germany, 8–10 September 1986; pp. 1107–1111.
3. Husain, T.; Hasan, I.; Sozer, Y.; Husain, I.; Muljadi, E. A Comprehensive Review of Permanent Magnet Transverse Flux Machines: Use in Direct-Drive Applications. *IEEE Ind. Appl. Mag.* **2020**, *26*, 87–98. [CrossRef]
4. Zhang, B.; Wang, A.; Doppelbauer, M. Multi-Objective Optimization of a Transverse Flux Machine with Claw-Pole and Flux-Concentrating Structure. *IEEE Trans. Magn.* **2016**, *52*, 8107410. [CrossRef]
5. Guo, Y.; Zhu, J.G.; Watterson, P.A.; Wu, W. Development of a PM Transverse Flux Motor with Soft Magnetic Composite Core. *IEEE Trans. Energy Convers.* **2006**, *21*, 426–434. [CrossRef]

6. EL-Refaie, A.M. Fractional-Slot Concentrated-Windings Synchronous Permanent Magnet Machines: Opportunities and Challenges. *IEEE Trans. Ind. Electron.* **2010**, *57*, 107–121. [CrossRef]
7. Cros, J.; Viarouge, P. Synthesis of High-Performance PM Motors with Concentrated Windings. *IEEE Trans. Energy Convers.* **2002**, *17*, 248–253. [CrossRef]
8. Weh, H. Permanentmagneterregte Synchronmaschinen hoher Kraftdichte nach dem Transversalflußkonzept. *ETZ Arch.* **1988**, *10*, 143–149.
9. Harris, M.R.; Mecrow, B.C. Variable Reluctance Permanent Magnet Motors for High Specific Output. In Proceedings of the Sixth Internet Conference on Electrical Machines and Drives, Oxford, UK, 8–10 September 1993; pp. 437–442.
10. Gieras, J.F. Performance Characteristics of a Permanent Magnet Transverse Flux Generator. In Proceedings of the IEEE Internet Conference on Electric Machines and Drives, San Antonio, TX, USA, 15 May 2005; pp. 1293–1299.
11. Maddison, C.P.; Mecrow, B.C.; Jack, A.G. Claw Pole Geometries for High Performance Transverse Flux Machines. In Proceedings of the Internet Conference on Electrical Machines (ICEM'98), Istanbul, Turkey, 2–4 September 1998; pp. 340–345.
12. Masmoudi, A.; Njeh, A.; Mansouri, A.; Trabelsi, H.; Elantably, A. Optimizing the Overlap Between the Stator Teeth of a Claw Pole Transverse-Flux Permanent-Magnet Machine. *IEEE Trans. Magn.* **2004**, *40*, 1573–1578. [CrossRef]
13. Sobczyk, T. Problemy modelowania matematycznego prądnic synchronicznych wzbudzanych magnesami Trwałymi. *Pr. Inst. Elektrotechniki* **2007**, *231*, 99–123.
14. Dreher, F.; Parspour, N. Reducing the Cogging Torque of PM Transverse Flux Machines by Discrete Skewing of a Segment-ed Stator. In Proceedings of the 21th International Conference on Electrical Machines, Marseille, France, 2–5 September 2012; pp. 454–457.
15. Gao, J.; Wang, G.; Liu, X.; Zhang, W.; Huang, S.; Li, H. Cogging Torque Reduction by Elementary-Cogging-Unit Shift for Permanent Magnet Machines. *IEEE Trans. Magn.* **2017**, *53*, 8208705. [CrossRef]
16. Zhu, L.; Jiang, S.Z.; Zhu, Z.Q.; Chan, C.C. Analytical Methods for Minimizing Cogging Torque in Permanent-Magnet Machines. *IEEE Trans. Magn.* **2009**, *45*, 2023–2031. [CrossRef]
17. Husain, T.; Hasan, I.; Sozer, Y.; Husain, I.; Muljadi, E. Cogging torque minimization in transverse flux machines. *IEEE Trans. Ind. Appl.* **2018**, *55*, 385–397. [CrossRef]
18. Junlong, L.; Yongxiang, X.; Jibin, Z.; Baochao, W.; Qian, W.; Weiyan, L. Analysis and Design of SPM Machines With Fractional Slot Concentrated Windings for a Given Constant Power Region. *IEEE Trans. Magn.* **2015**, *51*, 3401804. [CrossRef]
19. Skwarczyński, J.; Drabek, T.; Lerch, T. Maszyna Elektryczna Zaczepowa i Sposób Działania Maszyny Elektrycznej Zaczepowej. Polish Patent P.437412, 25 March 2021.